Carpathian Journal of Earth and Environmental Sciences, July 2017, Vol. 12, No. 2, p. 605 - 616

ESTIMATION THE EVAPOTRANSPIRATION OF URBAN PARKS WITH FIELD BASED AND REMOTELY SENSED DATASETS

Orhideja ŠTRBAC[1*], Miško MILANOVIĆ[1] & Vukan OGRIZOVIĆ[2]

[1]*University of Belgrade, Faculty of Geography, Studentski trg 3/III, 11000 Belgrade, Serbia sorhideja@gmail.com*

[2]*University of Belgrade, Faculty of Civil Engineering, Bulevar kralja Aleksandra 73/I, 11000 Belgrade, Serbia*

Abstract: Climate data and remote sensing images are used in this study to estimate the evapotranspiration of urban landscape vegetation. The study was conducted on a historic public park in Vršac (Serbia), which is an important Serbian national heritage site. After comparing recordings from 14 weather stations in the region with recordings from the City Park, the weather station in Vršac was chosen. The daily averaged values of climatic data for March, June, July and October of each year between 1949 and 2016, were used to compute the daily reference evapotranspiration ET_l (mm/day), according to the FAO-56 Penman-Monteith equation. A landscape coefficient was estimated through field monitoring based on the Water Use Classification of Landscape Species (WUCOLS) principles. Also, thermal infrared images from Landsat 8 and the Normalized Difference Vegetation Index (NDVI) from the QuickBird Satellite data are used as the remote sensing inputs to model daily evapotranspiration. This research explored the relationship between urban vegetation ET_l computed by the FAO-56 Penman-Monteith method with the required meteorological data and by means of the remote sensing. The analysis revealed the significant correlation between the average daily evapotranspiration estimates from 0.98 to 0.99 by the Nadaraya-Watson kernel regression and the weak Spearman's Rank correlation (**r** ranges from -0.006 to 0.384) leading to the conclusion that the Nadaraya-Watson kernel regression is more suitable for evaluating urban landscape water requirements.

Keywords: FAO-56 Penman-Monteith, remote sensing images, NDVI, WUCOLS, urban parks

1. INTRODUCTION

Due to the increased pressure on water supplies and concerns over the conservation of green areas in urban environments, it is important to estimate the water demands of various plants. Restoration of the oldest public park in Serbia, situated in Vršac, started in 2012. In order to develop a manageable irrigation design solution, the landscape evapotranspiration had to be estimated. The main objective of this paper is to quantify urban landscape evapotranspiration using meteorological and field survey data and remote sensing images, more specifically to investigate the statistical relationship between the Normalized Difference Vegetation Index (NDVI) and the estimated urban landscape evapotranspiration for one the biggest urban parks in Vršac. So far this is the first implementation of remote sensing to estimate evapotranspiration in urban parks in Serbia. Evapotranspiration is an important process within urban green areas, the rates of which are dependent upon temperature, vapour pressure and wind velocity. The Penman-Monteith method combined with Water Use Classifications of Landscape Species (WUCOLS) is often used to match the water requirements of plants. A common procedure for its estimation is the two-step approach: calculation of the reference evapotranspiration and then multiplication by the plants coefficients. Reference evapotranspiration is defined in (Allen et al., 1998) as "the rate of evapotranspiration from a hypothetical crop with an assumed crop height (0.12 m) and a fixed canopy resistance (70 s m^{-1}) and albedo (0.23) which would closely resemble evapotranspiration from the extensive surface of a green grass cover of uniform height, actively growing, completely shading the ground and not short of water".

The WUCOLS approach, confirmed in the field, is shown to be accurate and efficient in the evaluation of landscape water requirements

(Costello & Jones, 2014). The project was initiated and funded by the Water Use Efficiency Office of the California Department of Water Resources and provides evaluations of the irrigation water needs for over 3,500 taxa (taxonomic plant groups) for 18 reference evapotranspiration zones.

Evapotranspiration can be also indirectly estimated using remote sensing data by applying physical models such as the Penman–Monteith equation or by analysis of its relationship to vegetation indices and surface temperature (Petropoulos et al., 2009). This method has been selected in this research according the international standards and methodologies promoted by the Food and Agriculture Organization of the United Nation-FAO (Allen et al., 2005; 2006). Numerous researchers such as (Ortega-Farias et al., 1998; Todorović, 1999; Hussein, 1999; Ventura et al., 1999); Beyazgul et al., 2000; Lecina et al., 2003; Berengena & Gavilan, 2005; Lopez-Urrea et al., 2006; Gavilan et al., 2007; Trajković, 2009) indicate the reliability of the Penman - Monteith method (Frank, 2016). Except for the meteorological recordings for the August and October 1999 from the field and the meteorological stations in Serbia in the different time periods, the databases CARPATCLIM (Lakatos et al., 2013) and CLIMWAT (Thiemig et al., 2010) were also used. The thermal Infrared Sensor (TIRS) from Landsat 8 is important for mapping land surface temperature which is one of the parameters in the evapotranspiration calculation. Digital terrain is used to provide the elevation, slope and aspect data to compute net solar radiation and wind speed maps. For the generation of solar radiation map by module r.sun of GRASS GIS software (Neteler & Mitasova, 2004), as input parameters, a single value from albedo was applied, while Linke turbidity values were obtained at a monthly scale from the SoDa Webpage (Stackhouse et al., 2016). In 1922 Linke proposed coefficients to estimate clear sky radiation as the product of the optical thickness of water and a clear and dry atmosphere (Ineichen & Perez, 2002; (2008). This factor approximates the model of atmospheric absorption and scattering of the solar radiation under clear skies (Remund et al., 2003).

The NDVI method is often recommended as a useful indicator to study ET rates (Johnson & Belitz, 2012; Nouri et al., 2014; Islam, & Islam Mamun, (2015). Sobrino et al., (2012) list derived land surface emissivity from a comparison between the measured values and then estimated with the NDVI method. A near linear relationship between ET and NDVI was reported by Rossato et al., (2005). Nouri et al., (2014) also assessed the correlation between ground-based ET and remotely sensed ET using NDVI. The value of the vegetation index is critically dependent on the form of the data used to calculate it (Steven et al., 2003). Hence, the QuickBird high spatial resolution image is also used to extract NDVI and is compared with observational-based field estimations of the urban landscape ET.

2. MATERIALS AND METHODS

2.1. Study area

The study area is the City Park in Vršac, one of only a few well preserved historical public parks in Serbia, built in a mixed style (a combination of French formal and English landscape styles), which was a characteristic feature of Europe in the 18th century. It is trapezoid in shape and occupies an area of 66670 m^2, with the central coordinate at 45^O 07’ 08" N, 21^O 18’ 44" E. The area is temperate with an average annual rainfall of 659 mm and with a mean maximum temperature of 21.6 °C in July and cold winters with a mean minimum temperature of 0.3 °C in January (Gburčik, et al., 2004). The City Park is surrounded by both a wall and wrought iron fence and with five rustic gates. During the fieldwork, 107 plant species were identified and divided into 4 large groups: plants in the form of trees, bushes, vines and herbaceous plants. For the most common trees in the park, species coefficients are given in accordance with (WUCOLS) but adjusted to the local climate.

2.2. Meteorological data

Regarding the fact there is no weather station in the City Park in Vršac, necessary for the daily recordings of the needed parameters to calculate ET_o which could be compared with the results obtained using remote sensing, after analysing the results obtained from 14 meteorological stations in the region, for this study the meteorological stations in Vršac was selected.

To calculate ET_o in the City park in Vršac the measured values of temperature and humidity in August and October 1999 with digital thermometer and hygrometer were used, while wind speed was measured by Lambrecht anemometer set up to a height of 10 m on a vehicle for public lighting bulb replacement (Štrbac, 2004).

The correlation between daily values obtained for the aforesaid months in the City Park in Vršac and those calculated from the meteorological station in Vršac, Banatski Karlovac, Beograd, Timişoara and Novi Sad, has been examined by Spearman’s Rank correlation coefficients (McDonald, 2014).

Distances and azimuths between the City Park and meteorological stations in Vršac, Banatski Karlovac, Belgrade, Timişoara and Novi Sad are about a 2.6 km and 355 degrees, a 23 km and 250 degrees, an 86 km and 241 degrees, 72 km and 356 degrees and a 120 km and 275 degrees, respectively. The best correlation between ET_o in the City Park and weather stations in Vršac have been observed.

The mean monthly values obtained at the City Park in Vršac and corresponding values calculated for Beograd, Novi Sad and Timişoara from the climatic databases CLIMWAT which used the Penman Monteith method in the time series from 1961 to 2000 (Contreras et al., 2011), and for Timisoara, Oraviţa and Banioc from the CARPATCLIM database which applied Thornthwaite's method (Szalai et al., 2013; Antofie, et al., (2015) for the August and October 1999 were also compared. Oraviţa and Banioc are located at a distance from the City Park in Vrsac of 32 km and 30 km, while the azimuths are about 107 and 250 degrees, respectively.

Based on the average monthly values of evapotranspiration for the period 1966 to 1995 (Rajić, 2003) daily mean values were calculated for the August and October in the following cities in Serbia: Palić, Sombor, Vrbas, Bečej, Kikinda, Zrenjanin and Sremska Mitrovica, whose distances from the City park are about a 162, 190, 140, 115,105, 80 and 135 km respectively, with azimuths of a 313, 294, 292, 300, 321, 292 degrees and 264, respectively.

Table 1. Spearman's Rank correlation coefficients **r** between daily values obtained in the City Park in Vršac, the meteorological station in Vršac and the cities of Banatski Karlovac, Beograd, Timişoara and Novi Sad for the August and October of 1999.

Location	Month	**r**
City Park in Vršac	August 1999.	1
	October 1999.	1
Meteorological station in Vršac	August 1999	0.6193317
	October 1999.	0.8026439
Banatski Karlovac	August 1999	0.4784509
	October 1999.	0.7376840
Beograd	August 1999	0.5351174
	October 1999.	0.5546333
Timişoara	August 1999	0.3834784
	October 1999.	0.7058961
Novi Sad	August 1999	0.5121634
	October 1999.	0.7989628

The Two-Tailed Test of Population Mean with Unknown Variance was applied to compare the average values of the ET_o at those locations (Crawley, 2013). At a 0.05 significance level, the critical values were laid between -2.042272 and 2.042272. In addition to weather stations in Vrsac, Zrenjanin and Banatski Karlovac others show deviations from the range of the critical values in at least one of the analysed months. Although the obtained evapotranspiration for Zrenjanin showed a better correlation with the City Park, the weather station in Vrsac was selected because of its proximity to the City Park and was calculated for a longer period of time compared to Zrenjanin. The results are shown in the Tables 1 and 2.

Meteorological data have been recorded over the last 67 years at a weather station located at 83 m above sea level, at 45^0 08'39" N, 21^0 18' 20" E., which is about a 2.6 km distance from the Vršac City park. The Input parameters used for the ETo calculation by EtoCalc software were the monthly averaged: maximum and minimum air temperature (°C), dew point temperature (°C), wind speed (m/s) and actual duration of sunshine in a day (hour/day). The Penman–Monteith (PM) evapotranspiration (ET) equation predicts the rate of total evaporation and transpiration from the earth's surface using commonly measured weather data (solar radiation, air temperature, vapour content, and wind speed (Allen, et al., 2006). The form of the equation is:

$$ET_o = \frac{0.408 \cdot \Delta \cdot (R_n - G) + \gamma \cdot \frac{900}{T+273} \cdot U_2 \cdot (e_a - e_d)}{\Delta + \gamma \cdot (1 + 0.34 \cdot U_2)} \quad (1)$$

where ET_o is the reference evapotranspiration [mm day^{-1}], Δ is the slope of the saturation vapour pressure function [kPa $°C^{-1}$], R_n is the net radiation at the crop surface [MJ m^{-2} day^{-1}], G represents soil heat flux density [MJ m^{-2} day^{-1}], T is the mean daily air temperature at 2 m height [°C], U_2 is the wind speed at 2 m height [m s^{-1}], e_a is the saturation vapour pressure [kPa], e_d is the actual vapour pressure [kPa], $(e_a - e_d)$ represents the saturation vapour pressure deficit [kPa] and γ is the psychrometric constant [kPa $°C^{-1}$].

2.3. Field data

The water needs of landscape plantings can be estimated using the landscape evapotranspiration formula:

$$ET_l = K_l \cdot ET_o \quad (2)$$

where ET_{l1} is the landscape evapotranspiration [mm day^{-1}], K_l is the landscape coefficient [dimensionless], and ET_o is the reference evapotranspiration [mm day^{-1}]. K_l is determined by multiplying species, density and microclimate factors to determine the overall landscape coefficient (Nouri, et al., 2014).

Table 2. The results of the Two-Tailed Test of Population Mean calculated for the City Park in Vršac and the meteorological station in Vršac, Beograd, Novi Sad, Timişoara, Oraviţa, Banioc, Palić, Sombor, Vrbas, Bečej, Kikinda, Zrenjanin and Sremska Mitrovica

Location	Database	Month	**t**
City Park in Vršac	Calculated from field data in 1999.	August	0
		October	0
Meteorological station in Vršac	Calculated from station 1949-2016.	August	0.3093202
		October	1.391941
Banatski Karlovac	Calculated from station 1973-2016	August	-0.6186405
		October	1.391941
Beograd	Calculated from station 1949-2016.	October	1.391941
	CLIMWAT 1961-2000	August	0.9279607
		October	2.087912
	Calculated from station 1966-1995.	August	-2.783882
		October	-0.6959705
Timişoara	CLIMWAT 1961-2000	August	0.3093202
		October	2.087912
	CARPATCLIM 1999	August	0.3093202
		October	2.783882
Novi Sad	Calculated from station 1949-2016	October	2.087912
	CLIMWAT 1961-2000	August	0.6186405
		October	2.783882
Oraviţa	CARPATCLIM 1999	August	1.855921
		October	4.175823
Banioc	CARPATCLIM 1999	August	0
		October	2.783882
Palić	Calculated from station 1966-1995	August	-2.474562
		October	1.391941
Sombor	Calculated from station 1966-1995	August	-1.546601
		October	2.087912
Vrbas	Calculated from station 1966-1995	August	-1.546601
		October	1.391941
Bečej	Calculated from station 1966-1995	August	-2.474562
		October	1.391941
Kikinda	Calculated from station 1966-1995	August	0.3093202
		October	0.6959705
Zrenjanin	Calculated from station 1966-1995	August	0.3093202
		October	0
Sremska Mitrovica	Calculated from station 1966-1995	August	-0.6186405
		October	2.783882

Costello & Jones (1994; 2000; 2014) developed the landscape coefficient calculation as the product of three adjustment factors:

$$K_l = K_s \cdot K_{mc} \cdot K_d \qquad (3)$$

where K_s is the adjustment factor for a particular plant species [dimensionless], K_{mc} is the adjustment factor for shade or microclimate [dimensionless] and K_d as the adjustment factor for plant density [dimensionless]. WUCOLS IV provides evaluations of the irrigation water needs for over 3,500 taxonomic plant groups used in California landscapes divided into 6 climate regions. Species factors range from 0.1 to 0.9 and are divided into four categories of water demand, namely very low, low, moderate and high. To account for differences in microclimate influenced by nearby buildings, structures and pavements the microclimate factor was used. This factor varies from 0.5 to 1.4. The density factor K_d is used in the landscape coefficient formula to account for differences in vegetation density with values from 0.5 for sparse plantings to 1.3 for mature or densely planted

landscapes (Nouri, 2014).

After analysing the water needs of the most common species in the city park and their ecology, the coefficient K_s is corrected according to local climatic conditions (Štrbac, 2004; Radoglou et al., 2009; Cubino, et al., 2014; Ravazzi & Caudullo, 2016). Hence a species factor of 0.55 was assigned. A density factor of 1.3 was selected for the canopy coverage according to the total number and types of trees and their age. Considering the minor influences of the nearby hospital, stadium and another park with a pedestrian zone, a microclimate factor of 1 was chosen. The product of these three coefficients of 0.715 is the landscape evapotranspiration coefficient K_l which was allocated to the City Park in Vršac.

2.4. Satellite data

The QuickBird Standard bundle images were acquired on 2009-10-01 at 11:19 a.m. and consisted of one panchromatic image at 0.7-m resolution and one multispectral image at 2.8-m resolution at nadir. This commercial imaging satellite acquires 11-bit data in five spectral bands covering panchromatic (525-924 nm), blue (447-512 nm), green (499-594 nm), red (620-688 nm), and near-infrared (755-874 nm) wavelengths. Applying pan-sharpening techniques, a spatial resolution of a panchromatic image is assigned to multispectral channels (Johnson, 2014). A digital ortho-photo map and digital terrain model (DTM) of Vršac were created during the former aero-photogrammetric campaign of the location (Geokrulj, 2009) and they have been used for the ortho-rectification and resampling satellite images to output a ground sample distance of 0.6 m for panchromatic and 2.4 for multispectral channels. Both of the subset scenes were registered to the 2005 ortho-photo with 25 ground control points and 10 tie points in a Root Mean Square (RMS) of 0.32 pixel.

The raw multi-spectral satellite data in the form of digital numbers (DN) were converted to Top-of-Atmosphere Reflectance in three steps. First, conversion of the QuickBird products from radiometrically corrected image pixel values to band-integrated radiance is achieved with the following formula:

$$L_{Pixel,Band} = absCalFactor_{band} \cdot q_{Pixel,Band} \qquad (4)$$

where $L_{Pixel,Band}$ are top-of-atmosphere band-integrated radiance image pixels [W-m^{-2}-sr^{-1}], $absCalFactor_{band}$ is the absolute radiometric calibration factor [W-m^{-2}-sr^{-1}-count^{-1}] for a given band and is listed in the .IMD files, and $q_{Pixel,Band}$ are radiometrically corrected image pixels [counts].

Conversion from band-integrated radiance to band-averaged spectral radiance is performed using the following equation (Krause, 2005):

$$L_{\lambda_{Pixel,Band}} = \frac{L_{Pixel,Band}}{\Delta\lambda_{Band}} \qquad (5)$$

where $L_{\lambda_{Pixel,Band}}$ are top-of-atmosphere band-averaged spectral radiance image pixels [W-m^{-2}-sr^{-1}-μm^{-1}], $L_{Pixel,Band}$ are top-of-atmosphere band-integrated radiance image pixels [W-m^{-2}-sr^{-1}], and $\Delta\lambda_{Band}$ is the effective bandwidth [μm] for a given band.

The Top-of-Atmosphere Reflectance is computed according to the equation (Updike, & Comp, (2010):

$$\rho_{\lambda_{Pixel,Band}} = \frac{L_{\lambda_{Pixel,Band}} \cdot d_{ES}^2 \cdot \pi}{Esun_{\lambda_{Band}} \cdot \cos(\theta_s)} \qquad (6)$$

where $\rho_{\lambda_{Pixel,Band}}$ is the top-of-atmosphere planetary reflectance for a given band [dimensionless], $L_{\lambda_{Pixel,Band}}$ are top-of-atmosphere band-averaged spectral radiance image pixels [W-m^{-2}-sr^{-1}-μm^{-1}], d_{ES} is the Earth-Sun distance [AU] for a given image acquisition, π is the mathematical constant approximately equal to 3.14159 [dimensionless], $Esun_{\lambda_{Band}}$ is the band-averaged solar spectral irradiance [W-m^{-2}-μm^{-1}] for a given band, θ_s is the solar zenith angle [degrees] for a given product.

During the vegetation season, six thirty-meter resolution Landsat 8 products were used to compute NDVI and to evaluate the evapotranspiration in this study area. Landsat 8 carries two push-broom sensors: the Operational Land Imager (OLI) and Thermal Infrared Sensor (TIRS), both of which provide an improved signal to noise ratio and 12-bit radiometric quantization of the data. For producing a Normalized Difference Vegetation Index (NDVI), digital numbers of red and near-infrared bands were converted into reflectance.

$$\rho\lambda' = M_\rho \cdot Q_{cal} + A_\rho \qquad (7)$$

where $\rho\lambda'$ is the top-of-atmosphere planetary spectral reflectance, without correction for solar angle [dimensionless], M_ρ is the reflectance multiplicative scaling factor for the band, Q_{cal}l is the Level 1 pixel value in DN and A_ρ reflectance additive scaling factor for the band (Zanter, 2015).

When the scene-centre solar elevation angle in the metadata was chosen, the conversion to true TOA reflectance is:

$$\rho_\lambda = \frac{\rho'_\lambda}{\sin(\theta)} \quad (8)$$

where ρ_λ is the top-of-atmosphere planetary spectral reflectance, with a correction for solar angle [dimensionless] and θ is the solar elevation angle.

The Dark Object Subtraction (DOS1) was applied for the Landsat atmospheric correction which is incorporated in Semi-Automatic Classification Plugin for QGIS (Congedo, 2016), while the atmospheric correction for the satellite image of QuickBird have been performed by i.atcorr of GRASS GIS method that uses the 6S algorithm - Second Simulation of Satellite Signal in the Solar Spectrum (Neteler & Mitasova, 2004). The polygons boundaries of the City Park were isolated by applying r.mask command and then the resolution of these images is set up to 0.4 x 0, 4 m (11011 pixels), with the command r.resample in GRASS GIS.

The Ashtech MobileMapper 100 receiver with 45 channels and operating system Windows Mobile 6.5 was used for the positioning of ground control polygons for digitizing training areas. After importing the vector map, it was converted into a raster map by using v.to.rast command to generate a signature file with module i.gensigset. The land cover map which has been used for the creation of the emissivity raster was classified by i.smap module of GRASS GIS. The computed Kappa values from produced land cover maps were 0.89 for the QuickBird (2-4) and 0.70 for Landsat 8 multispectral bands (2-7). The land surface emissivity map from the masked QuickBird multispectral images was reclassified according to the review of the literature of emissivity (Salisbury, 1992; Sobrino et al., 2012; Ahire, (2013) from the oxidised tin roofs of the buildings in City Park (0.07), trees (0.99), green grass (0.97) and the pavements (0.83).

The thermal infrared channels were used as an alternative way to validate Penman-Monteith estimates of evapotranspiration. After the digital numbers for the thermal bands have been converted to radiance values, the inverse of the Planck function have been applied to derive an effective at-sensor brightness temperature (Chander et al., 2009):

$$T = \frac{K_2}{\ln\left(\frac{K_1}{L_\lambda}+1\right)} \quad (9)$$

where T is the effective at-sensor brightness temperature [K], K_2 is the calibration constant 2 [K], K_1 is the calibration constant 1 [W/(m^2 sr pm)] and L_λ is the spectral radiance at the sensor's aperture [W/(m^2 sr pm)].

The brightness temperature raster maps in °K were obtained from the thermal channels of Landsat 8 products by applying the inverse of the Planck function.

At-Satellite Brightness Temperature was converted from the Land Surface Temperature using the following equation (Weng et al., 2004):

$$S_t = \frac{T_b}{1+\left(\lambda \times {}^{T_b}/_{\rho}\right)\ln \varepsilon} \quad (10)$$

Where λ is the wavelength of emitted radiance, ρ = h x c/σ (1.43810 2 m K), σ is a Boltzmann constant (1.38 x 10^{-23} J/K), h is a Planck's constant (6.62610^{-34} J s), and c = velocity of light (2.998 x108 m/s).

For the T_b the brightness temperature raster maps were used, for the λ value from the Landsat Thermal Band 10 of 10.6 μm and for the ε emissivity raster. Finally, Land Surface Temperature maps in °C were obtained from calculated Land Surface Temperature maps in K subtracting 273.15.

Figure 1. Ortho photo of the City Park in Vršac from 2005.

2.5. Normalized Difference Vegetation Index (NDVI)

The normalized Difference Vegetation Index (NDVI) has been used extensively for the remote estimation of many important vegetation parameters for agricultural, ecological, and climate models (Johnson & Belitz, 2012; Johnson, 2014). The NDVI is the ratio between the maximum absorption of radiation in the red spectral band versus the maximum reflection of radiation in the near infrared spectral band:

$$NDVI = \frac{(\rho_{NIR}-\rho_{RED})}{(\rho_{NIR}+\rho_{RED})} \quad (11)$$

where ρ_{NIR} is the spectral reflectance measurements acquired in the near-infrared regions and ρ_{RED} is the spectral reflectance measurements acquired in the visible red regions.

For the QuickBird multispectral imagery, they are band 3 and band 4, but for Landsat 8, they are band 4 and band 5. After pre-processing described in the previous paragraph, $NDVI$s were calculated applying r.mapcalc (Shapiro & Westervelt, 1994). In order to exclude the areas of soil and buildings in the NVDIs a supervised classification was performed explained in the previous section. Then to the areas with no vegetation were assigned the null value using the logical operator in map algebra.

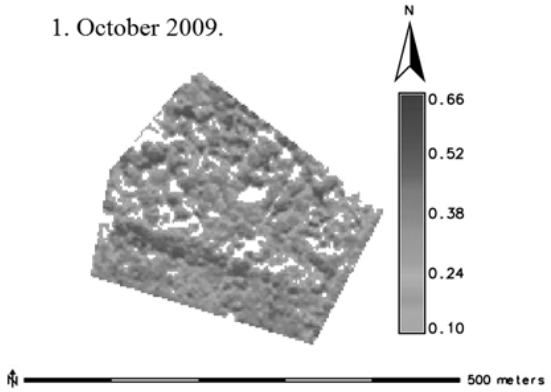

Figure 2. NDVI from the QuickBird image on 1st October 2009.

2.6. Ancillary data

The potential evapotranspiration calculation with hourly Penman-Monteith was computed by an i.evapo.pm algorithm implemented in GRASS GIS. The parameters needed for the calculation by this module are the elevation raster map, the temperature raster map in [°C], the relative humidity raster map [%], the input wind speed raster map [m/s], the net solar radiation raster map [MJ/m^2/h] and the crop height raster map [m].

The digital terrain model of 3 m x 3 m grid was an input parameter for this algorithm, the crop height raster map generation and for producing the wind speed raster map using the WindNinja, a computer program that computes spatially varying wind fields (Forthofer, 2007; Forthofer et al., 2014). The wind speed raster maps produced by WindNinja software (Wagenbrenner et al., 2016) were converted from miles per hour at a 10 meter height to meters per second at a 2 m height. The polygon which encompassing the boundaries of the City Park was isolated, then the vectors of wind speed were rasterised and were set up to the resolution of 0.4 x 0.4 pixels, like other input maps. Raster maps of slope and aspect, which is applied in the solar irradiance and irradiation model for the computation of direct (beam), diffuse and reflected solar irradiation raster maps, are also generated (Hofierka & Šúri, 2002). The net radiation raster input maps were produced by adding the three radiation components outputted by r.sun (beam, diffuse, and reflected solar irradiation raster maps) multiplied by the Wh to MJ conversion factor (0.0036). The temperature raster maps in °C were obtained from the thermal channels of Landsat 8 products by applying the procedure interpreted in the previous section of the paper. The relative humidity raster maps were computed by r.mapcalc commands according to the meteorological data recorded on those days when the six Landsat products were generated.

The Linke turbidity factor is defined as the number of clean dry atmospheres necessary to have the same attenuation of the extra-terrestrial radiation produced by the real atmosphere (Djelloul & Abdanour, 2013). In this research, the values of the Linke turbidity factor were obtained through the SoDa web service.

2.7. Relationship between NDVIs, ET_l from the meteorological and field data and the remote sensed ET_{lr}

The arithmetic means, standard deviation, range and variance for each input raster map of the particular month were extracted by the command of GRASS GIS r.univar. After a resampling of the ET_l from the meteorological data from 67 years to 11011 cells of the NDVIs and remote sensed ET_{lr}, the relationship between them was assessed by Spearman's Rank correlation coefficients. Considering a very weak correlation between Et_l adjusted from the meteorological data, the nonparametric regression by applying Nadaraya-Watson kernel estimators was also performed (Demir & Toktamiş, 2010). Finally, the same procedure was implemented to compare the averaged values of evapotranspiration by months after a bootstrapping (Fox & Weisberg, 2012) to 402 statistical means of the NDVIs and the ET_{lr}s from Landsat 8 images and an additional 67 from the calculated meteorological data for the examining a relation with the NDVI from the QuickBird satellite. Statistics were performed using R, a free software environment for statistical computing and graphics (Kerns, 2011).

Additionally, the level of agreement of Landsat images from the same months but different years were assessed by the Fuzzy Numerical (FN)

index. The FN index is computed as the average of the numerical similarity between each pair of corresponding cells values in the two maps (Avitabile et al., 2011) as follows:

$$s(a,b) = 1 - \frac{|a-b|}{max(|a|,|b|)} \qquad (12)$$

where $s(a,b)$ is the FN index, a and b are the corresponding cells in the two maps.

The daily mean values of ET_o for June and August are averaged from the Landsat 8 products acquired on three different years. Hence, the spatial similarity of these maps by the Fuzzy Numerical index is performed. The average values of 0.996 for June and 0.844 for August indicated a strong similarity between estimating evapotranspiration.

3. RESULTS

The most common plants in the City Park in Vršac have a habitus of trees out of which some 46 % belong to species with moderate, 12% with low and 8% with high requirements for water, according to the determined K_s. In order to calculate the weighted average, the percentage of these species in total number of trees is considered. A close up of the estimated landscape evapotranspiration during the study period is shown in Table 3.

Table 3. Averaged daily ET_o and ET_l in mm for the March, June, July August and October from recordings at Vršac meteorological station (1949-2016)

Month	March	June	July	August	October
ET_o	2.92	4.69	5.19	3.90	2.30
ET_l	2.089	3.357	3.714	2.786	1.643

NDVI was derived from the red and infrared channels of the six Landsat 8 products and the one QuickBird image, which were generated on 21th March 2014, 9th June 2014, 12th June 2015, 8th July 2013, 9th August 2013, 12th August 2014 and 1th October 2009, respectively.

The digital terrain model (DTM) was created from the ortho photo of the City Park in Vršac from 2005.

Daily 0.4-m ET_o data were created for the City Park in Vršac, Serbia, in GRASS GIS grid format and World Geodetic System 1984 (WGS84) datum, using the six Landsat thermal channels converted to land surface temperature. Because of the exclusion of non-vegetation areas, the NDVI from QuickBird bundle images had 1009 cells values less than the other rasters produced from Landsat 8.

The averaged values over 11011 cell values of ET_{lr} and NDVI from the Landsat 8 images and 10002 of the QuickBird NDVI are shown in the Table 4:

Table 4. Averaged daily evapotranspiration and NDVIs values from the Landsat 8 imagery

Date	ETlr	NDVI
07-08-2013	3.987	0.720
08-09-2013	4.239	0.682
03-21-2014	2.340	0.542
06-09-2014	4.349	0.740
08-12-2014	3.574	0.687
06-12-2015	4.356	0.757

The association between a remotely sensed ET_{lr}, NDVIs and ET_l from climatological data were evaluated by Spearman's Rank correlation coefficients (Mukaka, 2012) and the nonparametric regression by applying Nadaraya-Watson kernel estimators (Devroye, 1978; Aljuhani & Al turk, (2014). The results are presented in Tables 5 and 6.

After bootstrapping of the averaged values of evapotranspiration by months, the Nadaraya-Watson kernel regression over 402 training points of the NDVIs and ETl_r from the Landsat 8, over 469 ET_l from climatological data and 67 for the QuickBird NDVI was performed. Additionally, the relation between them was examined by the Spearman's Rank correlation coefficients. The results for R^2 and $\mathbf{r}$ are shown in Table 7.

4. CONCLUSIONS

Potential evapotranspiration at the City Park in Vršac, Serbia are estimated by three different approaches. From local-scale measurements, it was computed using the Penman–Monteith method by applying an adjusted landscape coefficient according to the WUCOLS methodology. The obtained mean daily ET_l varied from 1.643 in October, 2.786 in August, 2.089 in March, and 3.714 in July to 3.357 in June.

Six scenes of Landsat 8 products were used for its estimation by the land surface temperature retrieval from the inverse of the Planck equation-based method. The remotely sensed averaged ET_r for March, June, August and July are 2.340, 4.352, 3.987 and 4.297, respectively.

The mean values of 7 NDVIs calculated from those Landsat 8 products and one QuickBird multispectral image ranges from 0.542 for March to 0.740 for June.

The Nadaraya-Watson kernel regression and Spearman's Rank correlation were also applied for the resampled ET_l from climatological data and the products of the remote sensing.

Table 5. Spearman's Rank correlation coefficients **r** between the daily values obtained of the NDVIs, ET_l from the climatological data and ETl_r from the Landsat 8, and the QuickBird NDVI

Month	Date	**r** for ET_l and ETl_r	**r** for ETl_r and NDVI	**r** for ET_l and NDVI
August	08-09-2013	0.022	-0.372	-0.413
	08-12-2014	0.018	-0.455	-0.455
March	03-21-2014	0.014	-0.494	-0.002
June	06-09-2014	0.006	-0.508	0.006
	06-12-2015	0.006	-0.568	0.006
July	07-08-2013	0.009	-0.535	-0.535
October	10-02-2009	N/A	N/A	-0.009

Table 6. The Nadaraya-Watson kernel regression over 11011 training points of the NDVIs, ETl from the climatological data and ETlr from the Landsat 8, and over 10002 training points from the QuickBird NDVI

Month	Date	R^2 for ET_l and ETl_r	R^2 for ETl_r and NDVI	R^2 for ET_l and NDVI
August	08-09-2013	0.000	0.926	0.004
	08-12-2014	0.000	0.925	0.003
March	03-21-2014	0.000	0.883	0.001
June	06-09-2014	0.000	0.940	0.001
	06-12-2015	0.000	0.934	0.001
July	07-08-2013	0.000	0.923	0.000
October	10-02-2009	N/A	N/A	0.000

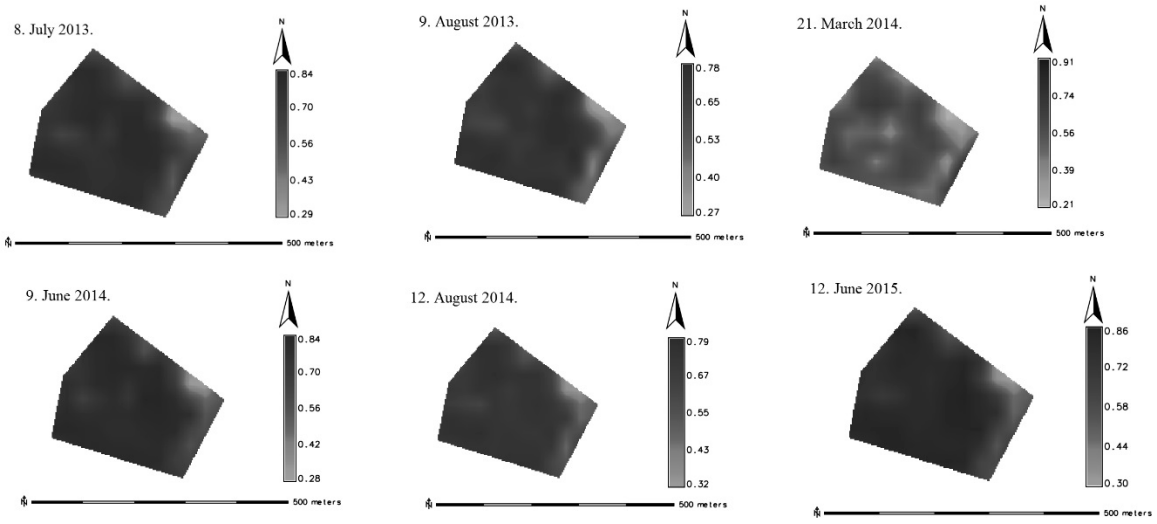

Figure 3. NDVIs of the study area from the Landsat 8 images

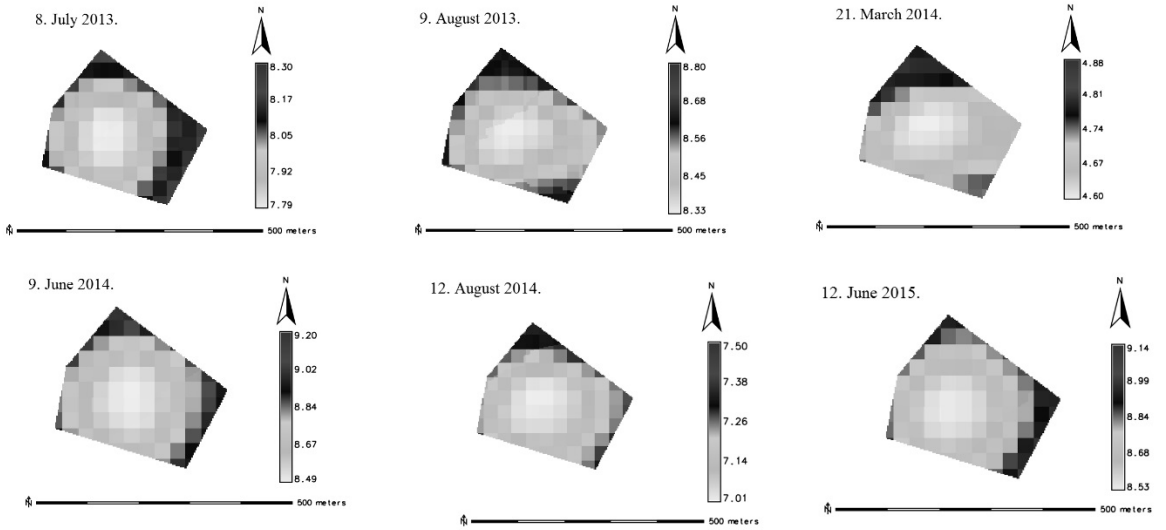

Figure 4. ET_{lr}s from the Landsat 8 images

Table 7. R^2 of Nadaraya-Watson kernel regression of the averaged values of evapotranspiration of the remote sensed products and the climatological data and Spearman's Rank correlation coefficients **r**

R^2 for ET_l and ETl_r	R^2 for ET_l and NDVI	**r** for ET_l and ETl_r	**r** for ET_l and NDVI
0.99	0.98	-0.006	0.384

Finally, the same procedure was performed over the average monthly values of evapotranspiration after bootstrapping of all needed data. However, using Spearman's Rank correlation, one of the results was negligible and the other moderate. This can be explained because of the different distribution of input data, the resampled Et_l from the climatological data for the period of 67 years from the one side and the bootstrapped ET_r and the NDVIs 11011 cell values of the remote sensing from the other side. This study showed the high positive correlation between ET_l and ET_r (R^2= 0.99) and NDVI and ET_l (R^2=0.98) by applying the Nadaraya-Watson kernel regression. The method quantified here which using remote sensing can provide reliable potential evapotranspiration estimates for the irrigation designs in other urban landscapes in Serbia.

Acknowledgments

We want to thank European Commission for the donation of a grant to the City of Vršac to implement an action of environment protection. The QuickBird image was acquired in 2009 due to this donation. Also, we want to thank Terance Payne, a teacher of English language for editing parts of the text.

REFERENCES

Ahire, D. V., 2013. Emissivity and scattering coefficient of tree leaves at 9.5 GHz frequency. Journal of Chemical, Biological and Physical Sciences, Vol. 3, No. 2, 1395-1403.

Aljuhani, H. K & Al turk, I. L., 2014. Modification of the adaptive Nadaraya-Watson kernel regression estimator. Scientific Research and Essays, Vol. 9 (22), pp. 966-971.

Allen, R., G., Pereira, L., Raes, D. & Smith, M., 1998. Crop evapotranspiration - Guidelines for computing crop water requirements - FAO Irrigation and drainage paper 56. FAO. Food and Agriculture Organization of the United Nations, Rome, 1-15.

Allen, R., G., Pereira, L., S., Smith, M., Raes, D. & Wright, J., L., 2005. FAO-56 Dual Crop Coefficient Method for Estimating Evaporation from Soil and Application Extensions. Journal of Irrigation and Drainage Engineering, Vol. 131. 2-13.

Allen, R., G., Pruitt, W., O., Wright, J., L., Howell, T., A., Ventura, F., Snyder, R., Itenfisu, D., Steduto, P., Berengena, J., Yrisarry, J., B., Smith, M., Pereira, L., S., Raes, D., Perrier, A., Alves, A., Walter, I. & Elliot, R., 2006. A recommendation on standardized surface resistance for hourly calculation of reference ET_o by the FAO56 Penman-Monteith method. Agricultural Water Management, 81(1-2), 1-22.

Antofie, T., Naumann, G., Spinoni, J. & Vogt, J., 2015. Estimating the water needed to end the drought or reduce the drought severity in the Carpathian region. Hydrol. Earth Syst. Sci., 19, 177–193.

Avitabile, V., Herold, M., Henry, M. & Schmullius, C., 2011. Mapping biomass with remote sensing: a comparison of methods for the case study of Uganda, Carbon Balance and Management, 6-7,1-14.

Berengena, J. & Gavilan P., 2005. Reference Evapotranspiration Estimation in a Highly Advective Semiarid Environment. Journal of Irrigation and Drainage Engineering, 131(2), 147-163.

Beyazgul, M., Kayam, Y. & Engelsman, F., 2000. Estimation methods for crop water requirements in the Gediz Basin of western Turkey, Journal of Hydrology, 229 (1-2), 19-26.

Chander, G., Markham, B. L. & Helder, D. L., 2009. Summary of Current Radiometric Calibration Coefficients for Landsat MSS, TM, ETM+, and EO-1 ALI Sensors. Remote Sensing of Environment, Manuscript Number: RSE-D-08-00684,1-24.

Congedo, L., 2016. Semi-Automatic Classification Plugin Documentation. Release 5.0.2.1- 1-198.

Contreras, S., Jobbágy, E., G., Villagra, P., E., Nosetto, M., D. & Puigdefábregas, J., 2011. Remote sensing estimates of supplementary water consumption by arid ecosystems of central Argentina. Journal of Hydrology, 397, 10-22.

Costello, L. R. & Jones, K. S., 1994. WUCOLS. WATER USE CLASSIFICATION OF LANDSCAPE SPECIES. A Guide to the Water Needs of Landscape Plants. California Department of Water Resources Water Conservation Office, Sacramento, California,1-96.

Costello, L. R. & Jones, K. S., 2000. A Guide to Estimating Irrigation Water Needs of Landscape Plantings in California. University of California Cooperative Extension, California Department of Water Resources. Sacramento, California. 1-160.

Costello, L. R. & Jones, K. S., 2014. Water Use Classification of Landscape Species. WUCOLS IV. University of California Cooperative Extension, California Department of Water Resources. Sacramento, California. 1-18.

Crawley, M. J., 2013. The R Book. Second Edition, A John Wiley & Sons, Ltd., Publication.1-975

Cubino, J. P., Subirós, J. V. & Lozano, C. B., 2014. Maintenance, Modifications, and Water Use in Private Gardens of Alt Empordá. Spain.HorTechnology 24,(3), 374- 383.

Demir, S. & Toktamiş, Ö., 2010. On the adaptive NADARAYA-WATSON kernel regression estimators. Hacettepe Journal of Mathematics and Statistics, Volume 39 (3), 429 – 437.

Devroye, L.P. 1978. The Uniform Convergence of the Nadaraya-Watson Regression Function Estimate. The Canadian Journal of Statistics, La Revue Canadienne de Statistique, Vol. 6, No. 2, 179-191.

Djelloul, D. & Abdanour, I., 2013. Estimation of atmospheric turbidity over Ghardaa city. Atmospheric Research, Elsevier, 2013, 128, 76-84.

Forthofer, J.M. 2007. MODELING WIND IN COMPLEX TERRAIN FOR USE IN FIRE SPREAD PREDICTION. Master thesis. Colorado State University. Fort Collins, Colorado. 1-123

Forthofer, J., M., Butler, B., W. & Wagenbrenner, N.S., 2014, A comparison of three approaches for simulating fine-scale surface winds in support of windland fire management. Part I. Model formulation and comparison against measurements, Int. J. Wildland Fire, 23,969-931

Fox, J. & Weisberg, S., 2012. Bootstrapping Regression Models in R. An Appendix to An R Companion to Applied Regression, Second Edition, 1-17.

Frank, A., 2016. Razvoj metodologije za procenu indikatora u cilju unapređenja prognoze klimatološke suše. Doktorska disertacija. Univerzitet u Novom Sadu. (in Serbian), 1-179.

Gavilan, P., Berengena, J. & Allen, R., G., 2007. Measuring versus estimating net radiation and soil heat flux: Impact on Penman-Monteith reference ET estimates in semiarid regions.Agricultural Water Management, 89, 275-286.

Gburčik, P., Gburčik, V. & Lazović N., 2004. Klimatski resursi opštine Vršac-preliminarna ocena stanja. Green Limes. Beograd, Serbia, (in Serbian),1-47, 374-383.

Geokrulj d.o.o, 2009. Final report of the contract realisation purchasing and processing of multispectral satellite images of Vršac Mountains' area. Belgrade, Serbia,1-8.

Hofierka, J. & Šúri, M., 2002. The solar radiation model for Open source GIS: implementation and applications. Proceedings of the Open source GIS - GRASS users conference 2002, September 2002, Trento, Italy,11–13.

Hussein, A., S., A., 1999. Grass ET Estimates Using Penman-Type Equations in Central Sudan. Journal of Irrigation and Drainage Engineering, 125(6), 324-329.

Ineichen, P. & Perez, R., 2002. A NEW AIRMASS INDEPENDENT FORMULATION FOR THE LINKE TURBIDITY COEFFICIENT. Solar Energy, Vol. 73, No. 3, 151–157.

Ineichen, P. & Perez, R., 2008. Conversion function between the Linke turbidity and the atmospheric water vapor and aerosol content. Solar Energy 82, 1095–1097.

Islam, M. & Islam Mamun, M., 2015. Variations of NDVI and Its Association with Rainfall and Evapotranspiration over Bangladesh. Rajshahi University Journal of Science & Engineering, Vol. 43, 21-28.

Johnson, B., 2014. Effects of Pansharpening on Vegetation Indices, ISPRS International Journal of Geo-Information. 2014, 3, 507-522.

Johnson, T. D. & Belitz, K., 2012**.** A remote sensing approach for estimating the location and rate of urban irrigation in semi-arid climates, Journal of Hydrology, 414–415, 86–98.

Kerns G. J., 2011. Introduction to Probability and Statistics Using R. First Edition, Youngstown State University, IPSUR, 1-395.

Krause, K., 2005. Radiometric Use of QuickBird Imagery-Technical Note. DigitalGlobe®, Longmont, Colorado, USA,1-18.

Lakatos, M., Szentimrey, T., Bihari, Z. & Szalai, S., 2013. Creation of a homogenized climate database for the Carpathian region by applying the MASH procedure and the preliminary analysis of the data. Quarterly Journal of the Hungarian Meteorological Service, Vol. 117, No. 1, 143–158.

Lecina, S., Martinez-Cob, A., Perez, P., J., Villalobos, F., J. & Baselga, J., J., 2003. Fixed versus variable bulk canopy resistance for reference evapotranspiration estimation using the Penman-Monteith equation under semiarid conditions, Agricultural Water Management, 60 (3), 181-198.

Lopez-Urrea, R., de Santa Olalla, F., M., Fabeiro, C. & Moratalla, A., 2006. Testing evapotranspiration equations using lysimeter observations in a semiarid climate. Agricultural Water Management 85(1), 15-26.

McDonald, J., H., 2014. Handbook of Biological Statistics. Third edition, University of Delaware, Sparky House Publishing, Baltimore, Maryland, USA, 1-305

Mukaka, M.M. 2012. Statistics Corner: A guide to appropriate use of Correlation coefficient in medical research. Malawi Medical Journal, 24(3), 69-71.

Neteler, M. & Mitasova, H., 2004. Open Source GIS: A GRASS GIS Approach.Second edition. KLUWER ACADEMIC PUBLISHER, NEW YORK, BOSTON, DORDRECHT, LONDON, MOSCOW, 1-417.

Nouri, H., 2014. Evapotranspiration estimation in heterogeneous urban vegetation. Doctoral thesis, University of South Australia, Adelaide, Australia, 1-192.

Nouri, H., Beecham, S., Anderson, S. & Nagler, P., 2014. High Spatial Resolution WorldView-2 Imagery for Mapping NDVI and Its Relationship to Temporal Urban Landscape Evapotranspiration Factors. Remote Sens. 2014, 6, 580-602.

Ortega-Farias, S., O., Barrias-Sanzana, R. & Cuenca,

R. H., 1998. Reference evapotranspiration by using the residual energy balance method. Proc. of Water Resources Engineering, ASCE, 1812-1817.

Petropoulos, G., Carlson, T.N., Wooster, M. J. & Islam, S., 2009. Progress in Physical Geography, 33(2). 224–250.

Radoglou, K., Dobrowolska, D., Spyroglou, G. & Nicolescu, V., N., 2009. A review on the ecology and silviculture of limes (Tilia cordata Mill., Tilia platyphyllos Scop. and Tilia tomentosa Moench.) in Europe. Die Bodenkultur, 60 (3), 9-19.

Rajić, M., 2003. Deficit vode u vodnom bilansu zemljišta Vojvodine. Letopis naučnih radova, Godina 27, broj 1, (in Serbian), 160–168.

Ravazzi, C. & Caudullo, G., 2016. Aesculus hippocastanum in Europe: distribution, habitat, usage and threats. European Atlas of Forest Tree Species, European Commission, Brussels, Belgium, 60-61.

Remund, J., Wald, L., Lefèvre, M., Ranchin, T. & Page, J., 2003. Worldwide Linke turbidity information. ISES Solar World Congress 2003, Göteborg, Sweden,1-14.

Rossato, L., Alvalá, R., C., S., Ferreira, N., J. & Tomasella, J., 2005. Evapotranspiration estimation in the Brazil using NDVI data. Proceedings of SPIE - The International Society for Optical Engineering, Remote Sensing for Agriculture, Ecosystems, and Hydrology VII, Vol: 5976, 358-367.

Salisbury, J. W., 1992. Emissivity of Terrestrial Materials in the 8-14 μm Atmospheric Window. REMOTE. SENS. ENVIRON, 42, 83-106.

Shapiro, M. & Westervelt, J., 1994. An Algebra for GIS and Image Processing. USACERL Techical report EC-94/13, 1-22.

Sobrino, J., A., Oltra-Carrió, R., Jiménez-Muñoz, J., C., Julien, Y., Sòria, G. & Mattar, C., 2012. Emissivity mapping over urban areas using a classification-based approach: Application to the Dual-use European Security IR Experiment (DESIREX). International Journal of Applied Earth Observation and Geoinformation, 18, 141–147.

Stackhouse, P., W., Chandler, W., S., Zhang, T., Westberg, D., Barnett, A. J. & Hoell, J. M., 2016. Surface meteorology and Solar Energy (SSE) Release 6.0 Methodology. NASA Langley Research Center-Hampton, VA, USA, 1-76.

Steven, M., D., Malthus, T., J., Baret, F., Xu, H. & Chopping, M. J., 2003. Intercalibration of vegetation indices from different censor systems. Remote Sensing of Environment, 88, 412–422.

Szalai, S., Auer, I., Hiebl, J., Milkovich, J., Radim, T., Stepanek, P., Zahradnicek, P., Bihari, Z., Lakatos, M., Szentimrey, T., Limanowka, D., Kilar, P., Cheval, S., Deak, Gy., Mihic, D., Antolovic, I., Mihajlovic, V., Nejedlik, P., Stastny, P., Mikulova, K., Nabyvanets, I., Skyryk, O., Krakovskaya, S., Vogt, J., Antofie, T. & Spinoni, J., 2013. CARPATCLIM Database © European Commission – JRC. Climate of the Greater Carpathian Region. Final Technical Report. www.carpatclim-eu.org.

Štrbac, O., 2004. Elementi funkcionalnosti Gradskog parka u Vršcu. Magistarska teza, Univerzitet u Beogradu, Serbia, (in Serbian),1-162.

Thiemig, V., Pappenberger, F., Thielen, J., Gadain, H., de Roo, A., Bodis, K, Del Medico1, M. & Muthusi, F., 2010. Ensemble flood forecasting in Africa: a feasibility study in the Juba–Shabelle river basin Atmos. Sci. Let. 11, 123–131.

Todorović, M., 1999. Single-Layer Evapotranspiration Model with Variable Canopy Resistance, Journal of Irrigation and Drainage Engineering, 125(5), 235-245.

Trajković, S., 2009. Metode proračuna potreba za vodom u navodnjavanju. Građevinsko-ahitektonski fakultet Univerziteta u Nišu, Niš, Serbia, (in Serbian). 1-110.

Updike, T. & Comp, C., 2010. Radiometric Use of WorldView-2 Imagery-Technical Note DigitalGlobe®. Longmont, Colorado, USA,1-16.

Ventura, F., Spano, D., Duce, P. & Snyder, R., L., 1999. An evaluation of common evapotranspiration equations. Irrigation Science, 18, 163-170.

Wagenbrenner, N.S., Forthofen, J. M., Lamb, B.K., Shannon, K.S. & Butler, B. W., 2016. Downscaling surface wind predictions from numerical weather prediction models in complex terrain with WindNinja. Atmos. Chem. Phys., 16, 5229–5241.

Weng, Q., Lu, D. & Schubring, J. 2004. Estimation of land surface temperature–vegetation abundance relationship for urban heat island studies. Remote Sensing of Environment, 89, 467–483.

Zanter, K. 2015. LANDSAT 8 (L8) DATA USERS HANDBOOK. Department of the Interior U.S. Geological Survey. Reston, VA, USA, 1-106.

Received at: 20. 07. 2016
Revised at: 03. 04. 2017
Accepted for publication at: 18. 04. 2017
Published online at: 24. 04. 2017